International Journal of Applied Pharmaceutics

ISSN- 0975-7058 Vol 16, Issue 2, 2024

Original Article

QUALITY BY DESIGN SUPPORTED CONSTRUCTION OF ORAL FAST-DISSOLVING FILMS FOR TELMISARTAN: RECONNOITERING THE QUALITY ATTRIBUTES

MEDISETTY GAYATRI DEVI[1*], SANTOSH KUMAR R.[2]

[1*]Gitam School Of Pharmacy, Gitam Deemed To Be University, Visakhapatnam, AP-530045, India. [2] Gitam School Of Pharmacy, Gitam Deemed To Be University, Visakhapatnam, AP-530045, India

[*]Corresponding author: Medisetty Gayatri Devi; [*]Email: gayatri.minnu@gmail.com

Received: 12 Dec 2023, Revised and Accepted: 31 Jan 2024

ABSTRACT

Objective: The angiotensin II receptor antagonist telmisartan (TMS) is often used to treat hypertension. The BCS class II antihypertensive drug TMS has a low solubility, poorly absorbed when taken orally. The goal of this study was to formulate an oral fast-dissolving film (OFDF) of TMS. In recent years, the concept of a rapidly dissolving dosage form as an innovative delivery system has gained popularity. By decreasing dosing frequency, maximize therapeutic effectiveness, bioavailability, and stability. It will also prevent the drugs from being metabolized in the first place. This technique allows for faster drug absorption from the gastrointestinal tract (GIT), which might result in a more rapid onset of action.

Methods: An experimental design known as Box-Behnken was employed to optimize a OFDF. Mango kernel (100-300 mg), maltodextrin (200-350 mg), and propylene glycol (PG) (15-30%) were chosen as independent variables with the highest preference. Included measurements of T5 tensile strength, disintegration time, folding endurance, elongation, and drug release efficiency as dependent variables.

Results: The physical properties of the films were found to be satisfactory, and Fourier transform infrared (FTIR) analysis failed to detect any drug-polymer interaction. F4 was found to have the greatest bioadhesive strength of 49.82 gm and the longest ex-vivo mucoadhesion duration of 189 min. A higher concentration of mango kernel in the formulation resulted in a greater rate of drug release. More than 60% of the drug was discharged within 10 min.

Conclusion: The oral mucosa of a rat was used for ex-vivo for irritation studies. Based on the pharmacokinetic plasma parameters, which is made into quick-dissolving films that are taken by mouth, is much better absorbed than aqueous suspensions. Studies of the enhanced formulation's stability showed that F4 may be stored for up to three months without deterioration.

Keywords: Telmisartan, Pharmacokinetic study, Mucoadhesion, Films, Solvent casting, *In vitro* studies, Ex vivo studies

DOI: https://dx.doi.org/10.22159/ijap.2024v16i2.50094 Journal homepage: https://innovareacademics.in/journals/index.php/ijap

INTRODUCTION

Fast-dissolving film (FDF) is a novel oral fast-dissolving dosage form that combines the benefits of being easy to administer and convenient to dissolve even when there is no water present [1]. As stated, "OFDF is relatively a new dosage form in which thin film is prepared using hydrocolloids, which rapidly dissolves on tongue or in buccal cavity" [2]. OFDF is a kind of film that may be used in the mouth without the need for a spoon. After the drug has been dissolved or disseminated in saliva, it may be ingested and absorbed normally. Rapid action may result from the absorption of certain drugs via the oral mucosa and into the GIT via the saliva. The drugs' bioavailability increases dramatically compared to when they were taken in tablet form [3]. For whatever reason, patients who struggle to swallow conventional tablets and capsules have sparked the quest for quicker-dissolving dosage forms, including a OFDF. People who have difficulty swallowing, including the elderly, kids whose internal muscles and central nervous systems are still developing, and traveller's who do not have easy access to water and have motion sickness and diarrhoea [4, 5]. Long-term patients who have frequent vomiting often have trouble swallowing. H2 blockers cannot be used by cancer patients who had chemotherapy [6, 7]. Because the drug has been diluted in saliva of the mouth, it is absorbed before it reaches the stomach. Drug absorption often occurs in the stomach, throat, and oral cavity. Pregastric absorption increases bioavailability by avoiding first-pass hepatic metabolism. Drug that is absorbed mostly in the mouth and the initial part of the GIT may have better safety profiles because first-pass hepatic and gastric metabolism produces less of the potentially hazardous metabolite [8–10].

A systolic blood pressure measurement of more than 140 mm Hg and a diastolic blood pressure measurement of more than 90 mm Hg are signs of hypertension [11]. Preventing the model drug's first-pass metabolism and accelerating the beginning of the drug's activity are the two objectives of OFDF preparation. Studies have shown that sublingual administration of TMS is preferable to oral administration of the drug since the latter is linked with side effects such as dry mouth, tiredness, and a hypotensive effect [12, 13], as well as swallowing difficulties [14]. Furthermore, it has been found that TMS administered sublingually is efficacious, easy, and safe [15, 16].

TMS has the best pharmacokinetic profile of all angiotensin II receptor antagonists, maintains blood pressure decrease for more than 24 h, and protects high-risk individuals from cardiovascular disease (CVD) [17, 18]. TMS is classified as a class II biopharmaceutical due to its physical features, which include low solubility in water and a dependence on pH [19]. Common strong alkalizers used in the preparation of commercial TMS formulations like Micardis® include sodium hydroxide, potassium hydroxide, and meglumine [20].

The preparation of pharmaceuticals has undergone a major shift in recent years [21]. A comprehensive knowledge of how process factors impact a product is achieved using the Quality by design (QbD) technique in pharmaceutical development [22]. The QbD definition provided by ICH (International Conference Harmonisation) Q8, quality-based development is "a systematic approach towards development that begins with predefined objectives and emphasizes product and process understanding and process control, based on sound science and quality risk management" [23]. "A dynamic product description that summarizes the quality characteristics expected to guarantee the product's performance, stability, safety, and efficiency" is the quality target product profile (QTPP), which is often used in the QbD process. The two main components of the QTPP are the critical quality attributes (CQAs),, and critical process parameters (CPPs). Characteristics that are suggestive of product quality CQAs may be retained, and CPPs are elements that impact CQAs. Combining CQAs and CPPs is ultimately makes design space explicable. It is possible to structure the preparation of OFDF and QTPP according to previously published research, considering the necessary

manufacturing requirements and characterization methods for achieving the required film characteristics. An OFDF that has been well prepared may be safely handled, is physically sound, and provides pleasant, straightforward service. Suitable organoleptic and mechanical features are two examples of how these characteristics might be interpreted into product quality [24].

This study's main goal was to formulate novel TMS-loaded OFDF that would increase drug bioavailability. In comparison to presently offered formulations on the market, QbD-based solubility and absorption improvements provide a comparable or even superior alternative. Additionally, a lot of emphasis is being paid to the fast drug onset that may be achieved via the sublingual and buccal routes with these TMS-loaded OFDF these days. The physicochemical characteristics of the optimized films were determined using differential scanning calorimetry (DSC) and X-ray diffraction (XRD). Numerous other properties of these films were also investigated, such as drug solubility, surface pH, folding endurance, tensile strength, and *in vitro* disintegration time.

MATERIALS AND METHODS

PG, citric acid, and aspartame utilized in this study were given by Modern Scientific Apparatus Pvt Ltd. in Hyderabad; maltodextrin (MDX) (dextrose equivalent 13.0-17.0) and PEG 400 were provided by Qualikems Fine Chem Pvt Ltd. Gattefosse India Pvt Ltd. supplied the mango kernel powder. Every one of the other compounds was of an analytical grade.

Experimental

Assigning of QTPP and CQA

The QbD approach was built on the precise selection and assignment of the QTPP, which included the proactive summary for obtaining the most value from the prepared product. The QTPP is used to identify critical process and formulation features to produce drugs that incorporate TMS-containing OFDF. To improve patient compliance and accelerate the advantages of drug, patient-centred therapy puts a high priority on the safe and effective administration of OFDF. The CPP for OFDF must be trustworthy, repeatable, and able to provide a product that meets all requirements. Based on the probability of risk and the degree of the related influence on the CQAs, categorized each CPP as high, medium, or low [25].

Risk assessment

To determined via risk assessment studies which critical material attributes (CMAs) and CPPs had the greatest impact on OFDF's CQAs. Fig. 1 presents an Ishikawa fishbone diagram that illustrates the possible high-risk elements that might impact the quality of the formulation. The specified features are important characteristics and/or factors for producing OFDF while employing TMS.

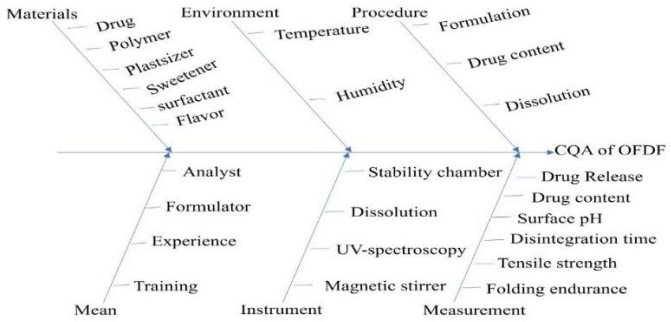

Fig. 1: Ishikawa fish-bone diagram depicting the cause-and-effect relationship among the formulation and process variables

High-performance liquid chromatography (HPLC) analysis of telmisartan

TMS content was ascertained using HPLC. Hitachi, Tokyo, Japan-made L-2130 pump, L-2420 UV-VIS detector, L-2350 column oven, L-2200 autosampler, and EZChromElite (version 3.1.8a) software made up the HPLC system. The column was a reverse-phase C18 Inertsil (IDS-3, 5 m, 15 cm, 4.6 mm) column. The mobile phase consisted of 5 mmol ammonium acetate and 0.45-M membrane-filtered methanol in distilled water (75:25). At a temperature of 25 °C, 20 l of the sample was added to the column. At a rate of 1 ml/min, the wavelength of the eluent was measured at 296 nm. All standard curves demonstrated high linearity with R^2 0.999 across the concentration range of 0.05-100 µg/ml, and the relative standard deviation was less than 3.6% in all concentrations and periods [26].

Design of experiment (DoE)

The purpose of a DoE is to measure the impact of various process characteristics on the efficacy of a formulation. This independent factors affected the dependent variables using a Box-Behnken design (BBD). The experiment was planned using Design-Expert 12.0.3.0 (State-Ease Inc., Version 12.0.3.0, Minneapolis, USA). Responses were examined in terms of tensile strength (mpa), folding endurance (mpa), disintegration time (s), elongation (%), drug release studies (Y4), and PG (%). Three independent variables (factors) were investigated: PG (%) (X3), maltodextrin (mg) (X2), and mango kernel (mg) (X1). To formulte of OFDF, preparatory experiments were used to choose the components (X1, X2, and X3) and determine their values. The many components used in the formulation of OFDF are shown in table 1 with the results of DoE experiments with well-stated dependent variables. Each batch of formulation underwent an independent series of experiments [27].

Table 1: Optimization variables and constrains used to TMS-OFDF using Box-Behnken design

Parameter	Low (-1)	Medium (0)	High (+1)
Independent variables			
X1: Mango Kernel (mg)	100	200	300
X2: MDX (mg)	200	275	350
X3:PG (%)	15	22.5	30
Dependent variables*			
Y1: Tensile Strength (Mpa)	1.26±0.36-8.96±0.51		
Y2: Disintegration Time (Sec)	15.34±1.13-46.35±1.24		
Y3: Folding Endurance (Folds)	124.7±1.62-395.6±1.46		
Y4: Elongation (%)	10.85±0.84-23.16±0.16		
Y5: % drug release T5 (min)	43.21±0.95-89.61±0.41		

*All the data are expressed as mean±standard deviation (n=3)

This design's efficacy was tested by creating and assessing 17 distinct formulations based on the same set of five "centre points". Quadratic, two-factor interaction (2FI), and linear models were used to fit the data for the dependent variable. A statistical regression analysis was also performed on the data obtained from each response [28]. Analysis of variance (ANOVA) was used to rank the models, and the top model was chosen. Three-dimensional graphs, contour plots, and polynomial equations were used to examine the parameters affected the formulation [29]. The polynomial equation that was developed to analyse various parameters affected the limitations was written as

$$Y = b0+b1A+b2B+b3\ C+b12AB+b13AC+b23BC+b11A2+b22B2+b33C2$$

A, B, and C are factor encodings; X is the intercept; Y is the response to each independent constraint; b_0 is the intercept; and b1 through b33 are regression coefficients based on actual experimental results. When two additional parameters are held constant, the solutions for each parameter are shown by the coefficients b1, b2, and b3. Changes in reaction due to simultaneous manipulation of both variables are represented by interaction terms (such as b12-b23). The preliminary screening phase may reveal independent constraints. By maximizing these values over 17 distinct formulations, the DoE produced the most common of which had five focus points. By feeding BBD information on the encapsulation efficiency (EE), particle size, and cumulative drug release of the formulations, were able to generate predicted values, polynomial equations, and model graphs. The analysis of the collected data allowed us to investigate the effects of external constraints on our dependent variables [30].

Preparation of OFDF

The OFDF used film production via the polymer's mango kernel and maltodextrin. PG was utilized as a plasticizer since MDX compositions without it are brittle. The process of solvent casting was used to make the films. The films were made using a drug-polymer solution of 10 ml. Polymers were dissolved in distilled water at the specified quantities, and the resulting solutions were stirred using a mechanical stirrer (Heidolph, Germany) for 2 h at a speed of 2000 rpm. After stirring for a further hour, the plasticizer was added to the mixture. At least 24 h of relaxation was required before using the dispersion to free out any trapped air. Each glass Petri dish was filled with the solution, which was then dried at 60 °C for two hours. After that, the completed film was dosed with DMS and sliced to the appropriate size. The research did not include any films that had cuts, air bubbles, or other defects [31].

Characterizations of TMS-loaded OFDF

Measurement of tensile strength

The mechanical quality was assessed using the model. Two clamps set at 3 cm apart were used to hold film strips that were a certain size and devoid of air bubbles or other physical flaws. The force was measured when the film ruptured after being compressed by the top clamp at a speed of 100 mm/min [32]. The tensile strength is calculated using the formula below:

$$\text{Tensile strength} = \frac{\text{Load taken to break the wire in newtons}}{\text{Cross sectional area mm2}}$$

Drug entrapment efficiency

To determine the film's EE, a 2 cm film was dissolved in 20 ml of pH 6.8 simulated saliva and shaken continuously for 30 min. Drug concentration in the solution was determined using UV spectroscopy at 296 nm [33, 34]. The entrapment rate was calculated using the following formula:

$$\text{Entrapment Efficiency} = \frac{\text{Total amount of drug added} - \text{amount of drug in supernatent}}{\text{Total amount of drug added}}$$

Disintegration time

When a film reaches this threshold, it begins to disintegrate in water. To calculate how long it would take for the target film to degrade completely, put it in a Petri dish with 25 ml of water and it dissolve within 30 sec [35, 36] is the optimum disintegration time.

Folding endurance

Folding a piece of film repeatedly in the same spot until it broke was used to determine could tolerate being repeatedly folded at an angle of 180 °. Folding endurance films with a rating of 300 or above are unusual [37]. A greater value for "folding endurance" [38] indicates that the film has more mechanical strength.

Surface pH

The pH of the oral cavity's surface was measured to assess the patient's tolerance for receiving OFDF. In a petri plate, OFDF was wetted for 60 sec with 0.5 ml of sterile water. The electrode was then touched to a pH meter to determine the acidity (or alkalinity) of the OFDF. OFDF works well at a surface pH between 6.8 and 7.4 [39].

Swelling index

Film swelling tests were evaluated using a saliva solution. The film was weighed on a digital analytical scale before being submerged in a pH 6.8 meant to mimic saliva. This procedure needed a petri dish, a plate glass, and the scale. Predetermined time intervals are recorded as the film's weight increases until there is no longer any rise in weight [40]. These factors then allow one to calculate the swelling index:

$$\text{Swelling Index} = \frac{Ws - Wd}{Wd}$$

ws = weight of film at time interval t (final weight), wd = weight of film at time 0 (initial weight).

Film thickness

Film thickness was typically measured using a micrometer screw gauge at 5 distinct spots throughout the film. Between 50-1000 mm is where you want to be for film thickness. The second research [41] agrees that a thickness of 0.3 mm or less for OFDF is still fine.

Weight uniformity

The weight uniformity test was carried out by weighing 20 units of OFDF at a size of 2 × 3 cm. The weight of the OFDF were tabulated and the results were expressed as the average weight±SD [42].

Solid state characterization

IR spectrum study

To investigate the potential drug-excipient interaction, FT-IR was performed. With an FT-IR spectrometer, were able to record the spectra of the pure drug, the film former, and the extruded films across a range of 4000 to 400 cm^{-1}. OFDF, film formers (Mango kernel, HPMC E 5, PEG 400, Aspartan, and optimal film), and TMS were investigated using FT-IR to identify drug-excipient interaction [43, 44].

Differential scanning calorimetry

The chosen optimum OFDF and its constituent solid components were subjected to DSC scans. Aluminum pans held the samples (3-5 mg) while the temperature was raised from 25 °C to 350 °C at a steady rate of 10 °C/minute. To obtained thermograms of the materials using DSC. Shimadzu TA 50I PC system and software were used to capture the thermal analysis data. The DSC temperature and enthalpy scale were calibrated using an indium standard. Nitrogen at a flow rate of 40 ml/min was employed as the purging gas [45, 46].

X-ray diffraction study (XRD)

XRD was used to analyze the crystalline behavior of the drug after it was developed. The crystal structures of TMS and film formers were determined using an XRD. The X-ray tube is a common place 40 kV 30 mA copper tube with a hermetically sealed design. Scanning at a rate of 4 °/min across a range of 2 was used to capture the XRD patterns [47, 48].

Morphology using scanning electron microscope (SEM)

The film was examined using a SEM to draw morphological findings. Using double-sided tape, the film was quickly attached to a metal rod. At 10 mA for 20 seconds, gold was deposited on the samples. At 15 kV, 1000x magnification is used to get surface morphology, whereas at 5 kV, 5000x magnification is used [49].

***In vitro* dissolution study**

An *in vitro* dissolution profile of OFDF of TMS was determined by whisking 900 ml of pH 6.8 simulated salivary fluid at 50 rpm in a USP

type 2 (basket device) at 37±0.5 °C for 20 min. A sample was obtained every 2 min, and the same amount of medium was thrown away and replaced with fresh medium. Using a UV spectrophotometer, the peak absorbance was determined to be at 296 nm. TMS pills were also compared to the produced formulation [50-52].

Ex vivo permeability study

Goat tissues were prepared and used in drug permeability tests. Saliva solution (pH 6.8) was freshly prepared and placed in the receptor compartment of a Franz diffusion cell. The epithelial side of the recently removed tissue was clamped towards the donor compartment. All the trials of were conducted at ambient temperature. Each group of samples was taken 30 min apart. The sample volumes were discarded after each collection and refilled with new media. UV spectroscopy at a maximum of 296 nm was used to calculate the concentration of drug in the release medium. The release trials were performed three times for each sample and the average results were recorded. The drug's calibration curve in the pH 6.8 salivary solution was used to determine the percentage of drug release [53, 54].

***In vivo* pharmacokinetic study**

The protocol for this research was reviewed and approved by the Institutional Animal Ethics Committee at Jeeva Life Sciences in Uppal, Hyderabad, India (Approval: CPCSEA/IAEC/JLS/011/11/22/15).

Animal dosing and sampling scheme

Sublingual administration of the optimal TMS-OFDF was compared to oral administration of the commercial tablet Telnosis® (40 mg TMS) in plasma samples from healthy rabbits. Fifteen rabbits were used, all of which were healthy and weighed between 1.25 and 2.25 kg. After fasting for 24 h, the rabbits were euthanized with 0.1 ml of thiopentone (0.5 mg/ml). The dosage used was around 40 mg/person or 2.5 mg/kg. The therapeutic dosage for humans was multiplied by a formula using a database of surface area ratios of common laboratory animals and humans to determine the dose administered to rabbits [55, 56]. This equation was applied:

$$Dr = Dh\ (Wr/Wh),3/4$$

where Dr is the dosage given to a rabbit, Dh is the dose given to a human, Wr is the weight given to a rabbit, and Wh is the weight given to a human [57, 58]. Random groups of rabbits (n=3) were assigned to receive either TMS commercial oral tablets (by stomach intubation), the TMS OFDF (via sublingual administration), or oral in pure drug solution (via oral administration). Before giving the drug to the rabbits, blood samples were obtained as a control. Before and at 0.5, 2, 4, 6, 8, 10, 12, 24, and 30 min following drug delivery, multiple blood samples (1-2 ml) were collected in heparinized vacutainer tubes. Plasma was obtained using centrifugation and stored in a freezer at 20 °C until analysis [59].

Analysis of plasma samples

The concentration of TMS in the plasma was determined using a sensitive HPLC technique, as described in the literature. The precise concentration of TMS was calculated using HPLC. An L-2130 pump, L-2420 UV-VIS detector, L-2350 column oven, and L-2200 autosampler from Hitachi, Tokyo, Japan, were used in conjunction with EZChromElite (version 3.1.8a) software to form the HPLC system. The C18 reverse-phase column manufactured by Inertsil (IDS-3, 5 m, 15 cm, 4.6 mm) was used. The mobile phase consisted of 75% distilled water, 5% ammonium acetate, and 0.45% membrane-filtered methanol. At 25 °C, 20 µl of the sample were poured into the column. At a flow rate of 1 ml/min, the eluent was measured at 296 nm. The relative standard deviation was less than 3.6% across all concentrations and periods, indicating good linearity with R^2 0.999 from 0.05 to 100 µg/ml [26]. Three replicates of each reference sample were analyzed.

Pharmacokinetics analysis

TMS's pharmacokinetics by tracking plasma concentrations over time using Win Nonlin standard version 1.5. Absorption rate constant (Ka), half-life of absorption (t12a), elimination rate constant (Kel), and half-life of elimination (t2) were determined for plasma MT concentrations over time (AUC). It was clear that the Cmax and Tmax were determined. Two indicators of effectiveness are the time it takes to reach a maximum concentration (Cmax) and the maximum concentration of time (Tmax). Areas under the curve (AUCs) may be compared between extravascular and intravenous delivery to determine the absolute bioavailability of a drug.

Statistical analysis

Unless otherwise specified, all experiments were run in triplicate. GraphPad Prism 6.0 (GraphPad Software, San Diego, CA, USA) to perform one-way analysis of variance and two-tailed Student's t-tests for comparisons across groups in the experiment. A P-value>0.05 indicates there is no statistically significant difference between the means being compared. Significant (S) and highly significant (HS) deviations from the mean were defined as 0.05>P0.01 and 0.01>P0.001, respectively, for the parameters.

RESULTS AND DISCUSSION

Using a QbD strategy, look at TMS-OFDF's CQAs. Priority was given to the formulation factors that have the greatest impact on film quality. As a result, know that the thickness of the film, the folding durability, the disintegration duration, and the drug dissolution are all critical quality attributes of TMS-OFDF. To determine how each independent variable affected the outcomes of interest, a screening method.

Quality target product profile

QTPP was utilized to zero down on the most crucial quality features and OFDF for TMS administration. Hypertension, often known as high blood pressure, is managed and treated by TMS-OFDF. QTPP of TMS includes the efficient and risk-free delivery of OFDF, which speeds up the onset of drug effects and increases patient adherence. The method used to make OFDF was stable and repeatable, therefore, the finished product had all the qualities required of a pharmaceutical-grade. The QTPP is listed in table 2, along with an explanation of why they were chosen [60].

Table 2: Quality target product profile (QTPP) earmarked for fast-dissolving oral film of TMS

QTPP	Target	Justification
Dosage form	Oral fast-dissolving Film	Similar dose forms are required in the pharmaceutical industry.
Route of administration	Oral cavity	To improve drug solubility and avoid first-pass metabolism, TMS should be administered subcutaneously.
Dosage Type	Oral film	Improved therapeutic efficacy due to a quicker beginning of action.
Packaging	Polyethylene strip	Same packaging requirements for pharmaceuticals
Stability	At least 90 d at room temperature	In order for the drug's therapeutic potential to be preserved over the required storage time.
Alternative routes of administration	None	There is no alternative delivery system.

Construction of ishikawa diagram

An Ishikawa diagram was created to help structure the risk analysis process of determining the major and secondary elements driving CQAs. To determine which characteristics of raw materials and manufacturing processes are most important to OFDF's quality, a risk analysis. Fig. 1 is an Ishikawa diagram depicting a cause-and-effect relationship between possible parameters impacting CQAs of

OFDF in TMS-OFDF. Some formulation parameter concentrations, such as X1, X2, and X3, are important due to the considerable risk they pose to certain key quality characteristics in risk assessment studies. The Y1-Y5 is the tensile strength, the second is the disintegration time, the third is the folding endurance, the fourth is the elongation, and the fifth is the drug release research. The OFDF was prepared without the use of any sophisticated laboratory apparatus, and no complicated process parameters were observed to significantly affect the formulation at any stage of the studies. However, the concentrations of a few formulations' characteristics were kept constant since they were judged to pose little to no harm. These were HPMC E5, PEG 400, and aspartame.

Optimization of formulations

Model building and statistical significance test

The end product of every recipe was a flexible film. The response surface was fitted using a BBD with three independent variables, three levels, and five center replicates [61]. These five trials were included to assess the repeatability and intrinsic degree of variation in the method. Design-Expert software was used to assess the experimental design outcomes (table 3), which yields insightful information and makes it simpler to replicate the statistical design for performing experiments.

Table 3: Experimental design and formulation variables of TMS-OFDF

Std	Run	X1	X2	X3	Y1*	Y2*	Y3*	Y4*	Y5*
1	17	100	200	22.5	6.59±0.53	20.13±1.02	186.2±2.35	16.52±0.13	73.51±0.29
2	13	300	200	22.5	3.26±0.41	16.35±1.31	395.6±1.46	21.86±0.42	60.48±0.85
3	5	100	350	22.5	5.42±0.26	21.84±1.41	283.4±2.03	19.62±0.35	64.72±0.75
4	4	300	350	22.5	8.96±0.51	15.34±1.13	354.9±1.43	23.16±0.16	89.61±0.41
5	8	100	275	15	1.34±0.38	46.35±1.24	124.7±1.62	10.85±0.84	43.21±0.95
6	16	300	275	15	3.85±0.17	26.35±1.05	213.8±1.42	18.53±0.47	56.39±0.52
7	12	100	275	30	3.02±0.42	18.93±0.95	134.4±1.09	11.86±0.23	63.25±0.31
8	6	300	275	30	3.16±0.16	18.43±0.52	279.4±0.98	13.48±0.31	59.02±0.75
9	9	200	200	15	2.69±0.35	37.05±0.75	167.6±3.1.2	12.96±0.24	49.86±0.62
10	15	200	350	15	4.59±0.42	41.26±0.42	195.7±2.42	20.54±0.15	53.29±0.42
11	11	200	200	30	2.19±0.12	23.06±0.98	186.9±1.68	16.27±0.52	56.24±0.35
12	7	200	350	30	5.48±0.15	20.48±1.32	259.8±2.41	16.05±0.13	77.04±0.42
13	3	200	275	22.5	1.29±0.53	21.52±1.42	157.4±1.69	17.53±0.85	76.84±0.48
14	2	200	275	22.5	1.43±0.42	29.04±1.26	160.5±1.52	16.59±0.92	78.32±0.75
15	1	200	275	22.5	1.26±0.36	35.62±1.42	158.2±1.74	18.52±0.42	73.26±0.49
16	14	200	275	22.5	2.51±0.41	34.62±0.52	148.8±1.59	16.92±0.41	77.03±0.62
17	10	200	275	22.5	3.48±0.28	29.31±0.62	139.4±1.42	14.03±0.69	75.14±0.45
1	17	100	200	22.5	6.59±0.41	20.13±0.94	186.1±2.03	16.52±0.43	73.51±0.95
2	13	300	200	22.5	3.26±0.39	16.35±0.85	395.5±1.42	21.86±0.75	60.48±0.43

*All the data are expressed as mean±standard deviation (n=3)

Mechanical properties

An ideal film formulation would not be only physically robust, but also adaptable, simple to use, and quick to administer. A high tensile strength [62] explains these features. The tensile strength of sublingual films as a function of polymer and plasticizer concentrations is shown in fig. 2. According to (Supplementary table 1) of the supporting materials, the model has statistical significance with a Prob>F value of 11.02. Important model words were X1, X2, X1X2, and X12. The F-value of 11.02 indicates that the model is significant statistically. Such a high F-value would only happen by chance 0.23% of the time. Statistical significance is assumed when a model term's p-value is less than 0.05. Model words B, AB, A^2, and B^2 play a key role in this context. Lack of Fit and pure error both have F-values of 0.29, indicating that there is no statistically significant difference between the two. A Lack of Fit F-value as large as this one is 82.89% attributable to chance. With an adjusted R^2 of 0.8493, we are within 0.2% points of our expected R^2 of 0.7250. The S/N ratio is determined with the help of Adeq Precision. When the ratio is more than 4, it seems favorable. An acceptable signal-to-noise ratio of 12.175%. More design options may be explored with this model. In terms of tensile strength, this is the gold standard:

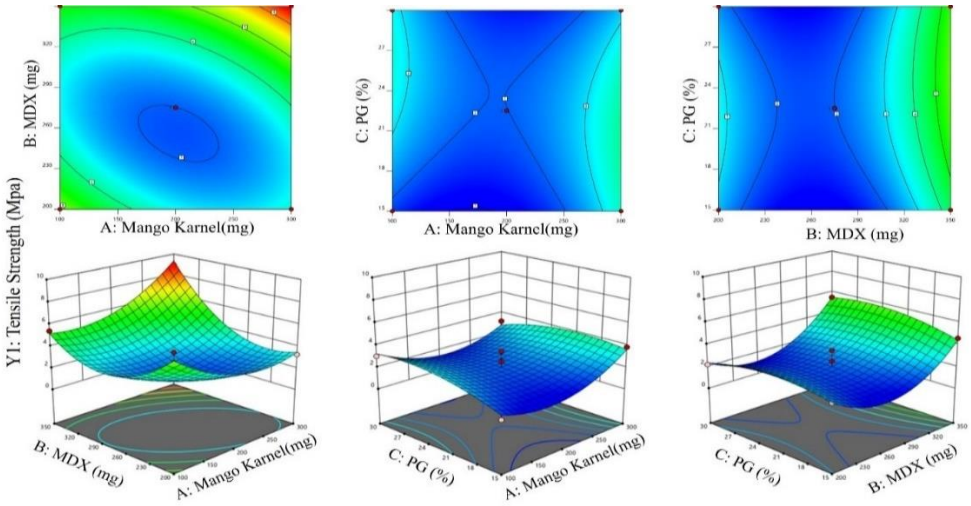

Fig. 2: Counter and Response-surface-methodology plot for the effect of formulation factors (X1, X2, and X3) on the Tensile strength (Y1)

Tensile strength =+1.99+0.3575A+1.22B+0.1725C+1.72AB-0.5925AC+0.3475BC+1.58A2+2.48B2-0.7357 C2

The tensile characteristics of MDX and mango kernel were compared, and it was shown that the ratio of these two polymers considerably (p≥0.05) altered the tensile strength of sublingual films. It has been shown that PG has a plasticizing impact on bio-polymers [63]. It is generally accepted that PG acted as a lubricant between the polymer chains, allowing for greater molecular mobility [64]. However, several ratios did not show a statistically significant change (p>0.05). OFDF of TMS that had been produced showed a tensile strength between 1.26±0.36-8.96±0.51Mpa. Optimized (F4) formulation tensile strength is shown in fig. 2. One of the most important aspects of OFDF is increasing its tensile strength. The tensile strength characteristics of OFDF would be affected by the kind and quantity of plasticizer and film-forming polymer used. OFDF with a higher plasticizer content, has a higher tensile strength and greater flexibility. According to the results, the tensile strength increased with increasing concentrations of X1, X2, and X3. However, the role played by X3, which makes OFDF more elastic and less brittle, was considered more important.

Effect of formulation factors on disintegration time

F = 6.87 and p≥0.05 indicate that the model is statistically significant. X1 and X12 are both important here as model variables (p≤0.05 for both). The drug quickly dissolves into its environment after the first burst of disintegration. This approach does not work well for hydrophobic drugs. A rapid rate of disintegration is particularly important for DMS, a hydrophobic drug. Fig. 3 shows that the amount of MDX in a sample affects how long it takes to disintegrate. Increases in MDX concentration were shown to result in thicker films. Because thicker films are more resistant to water penetration than thinner films, those with a higher concentration of MDX were shown to have longer disintegration durations. The model is statistically significant with an F-value of 6.87. An F-value so high can only occur by chance 0.94% of the time. Statistical significance is assumed when a model term's p-value is less than 0.05. Model terms A, C, and especially A^2 are critical. There is no statistically significant difference between the Lack of Fit and randomness, as shown by the F-value of 0.14. A Lack of Fit F-value as large as this one is 93.13% likely to be attributable to random chance. Differences between the expected R^2 of 0.7019 and the modified R^2 of 0.7674 are small (less than 0.2). The S/N ratio is determined with the help of Adeq Precision. When the ratio is more than 4, it seems favorable [65]. According to (Supplementary table 2), your signal-to-noise ratio seems to be satisfactory at 9.004.

Disintegration Time =+30.02-3.85A+0.2913B-8.76C-0.6800AB+4.88AC-1.70BC-7.28A2-4.33B2+4.77C2

When it comes to fast-acting oral films, disintegration time (DT) is a useful indicator [66]. All of the TMS-OFDF had a DT of less than 46.35±1.24 sec, meeting the criteria specified elsewhere. Higher levels of DT (Y2) were shown to be affected by all three parameters (X1, X2, and X3). Fig. 3 shows a scatter plot illustrating the impact of various factors on the disintegration time (s). The disintegration period of OFDF will be controlled by taking these parameters into account. However, films made from X1 and X3 at high concentrations would meet a criterion for rapid disintegration.

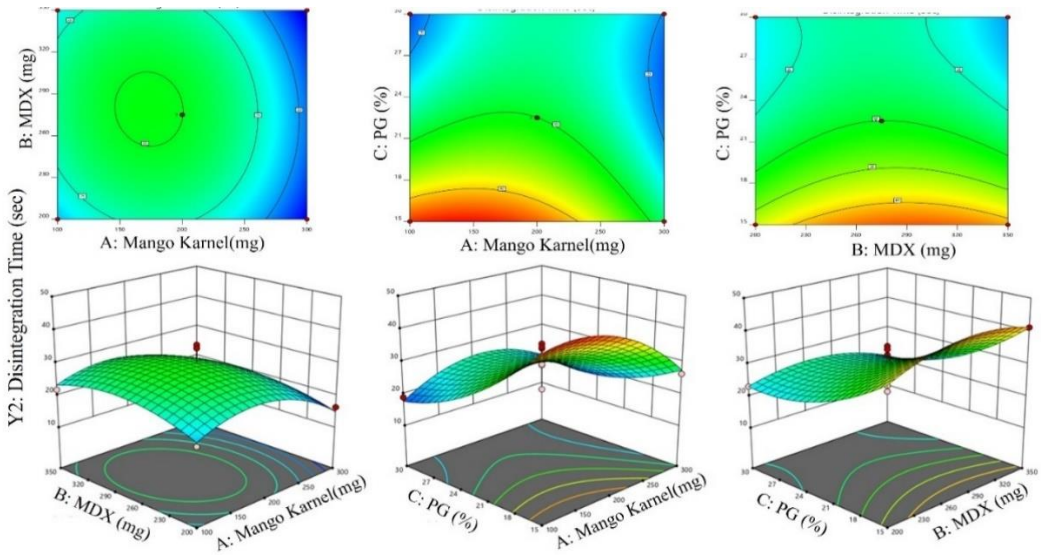

Fig. 3: Effect of formulation variables (X1, X2, and X3) on disintegration time (Y2), as plotted by the counter and response surface methodology

Effect of formulation factors on folding endurance

The strong mechanical strength and good flexibility of all the TMS-OFDF are on display in their folding endurance of 124.7±1.62 to 395.6±1.46 times (no). The plasticizer and film former work together to give the film its pliability and strength, respectively. Therefore, an OFDF with ideal quality may be achieved by concentrating both components to the right degree. According to the findings, mango kernel, MDX, and PEG 400 all contribute positively to folding endurance. Mango kernel's ability to relax linear polymeric chains, maybe via the creation of hydrogen bonds, increases flexibility and folding durability. The study's findings about the relative benefits of Mango kernel, MDX, and PEG 400 for prolonged folding are shown in fig. 4. Below, we define the polynomial term for folding endurance [67].

Folding Endurance =+152.40+64.25A+19.63B+19.88C-34.50AB+14.00AC+11.25BC+68.92A2+83.17B2-33.82C2

An F-value of 93.25 indicates the model is statistically significant. The chance of such a high F-value occurring by chance is less than 0.01%. Statistical significance is assumed when a model term's p-value is less than 0.05. A, B, C, AB, AC, A2, B2, and C2 are all instances. With an F-value for Lack of Fit of just 2.26, it is unlikely that this phenomenon can be distinguished from chance. There is a 22.38% possibility that such a large F-value for Lack of Fit is just coincidental. Adjusted R^2 0.9811, which is consistent with Predicted R^2 0.9120; the difference between the two is smaller than 0.2. The S/N ratio is determined with the help of Adeq Precision. When the ratio is more than 4, it seems favorable. Your signal-to-noise ratio of 31.824 is satisfactory (Supplementary table 3).

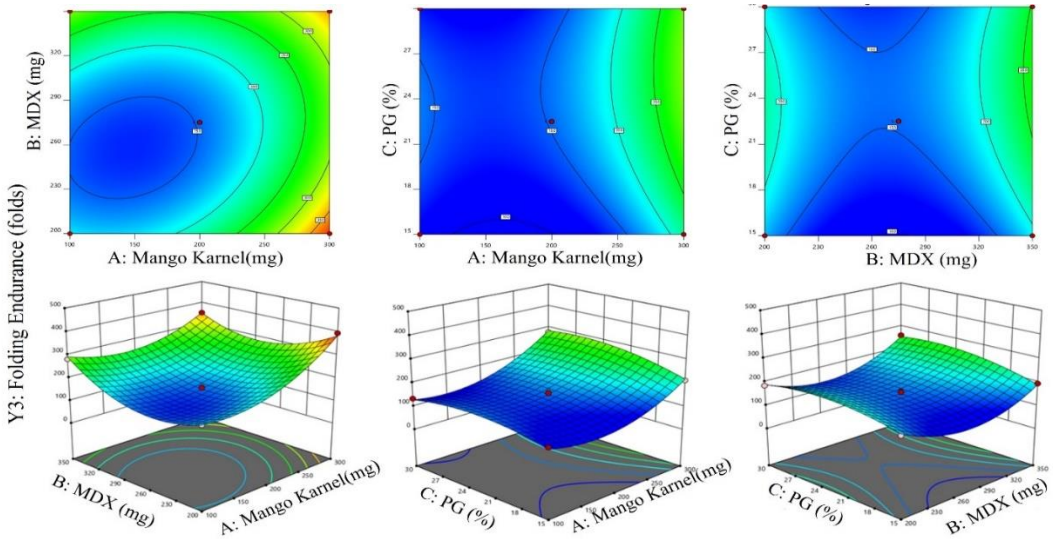

Fig. 4: Counter and response-surface-methodology plot for the effect of formulation factors (X1, X2, and X3) on the folding endurance (Y3)

Effect of formulation factors on elongation

The length of a film is an essential metric for evaluation. Elongation increases the film's durability and the drug-absorbing surface area. It also has the potential to allow for a more rapid rate of release. The films' elongation was measured to be between 10.85±0.84 to 23.16±0.16%. According to the derived quadratic model, the Tensile Strength is significantly impacted by the X1, X2, and X3 amounts. The predicted values were rather close to the actual values (fig. 5).

Elongation =+16.72+2.27A+1.47B-0.6252C-0.4500AB-1.52AC-1.95BC+0.3985A2+3.17B2-3.44C2

With an F-value of 10.23, the model has high statistical support. A random F-value this high only happens 0.29% of the time. Statistical significance is assumed when a model term's p-value is less than 0.05. Important illustrative ideas are denoted by the A, B, BC, B2, and C2. The Lack of Fit F-value is just 0.25, thus, it's not much different from just plain old mistakes. An F-value of 0.8547 for Lack of Fit is statistically significant. The discrepancy between the adjusted R^2 of 0.8385 and the predicted R^2 of 0.7259 is small (less than 0.2). The S/N ratio is determined with the help of Adeq Precision. When the ratio is more than 4, it seems favorable. Your signal-to-noise ratio of 12.319 is quite high. To examine how this model compares to others, check out (Supplementary table 4) in the Materials List.

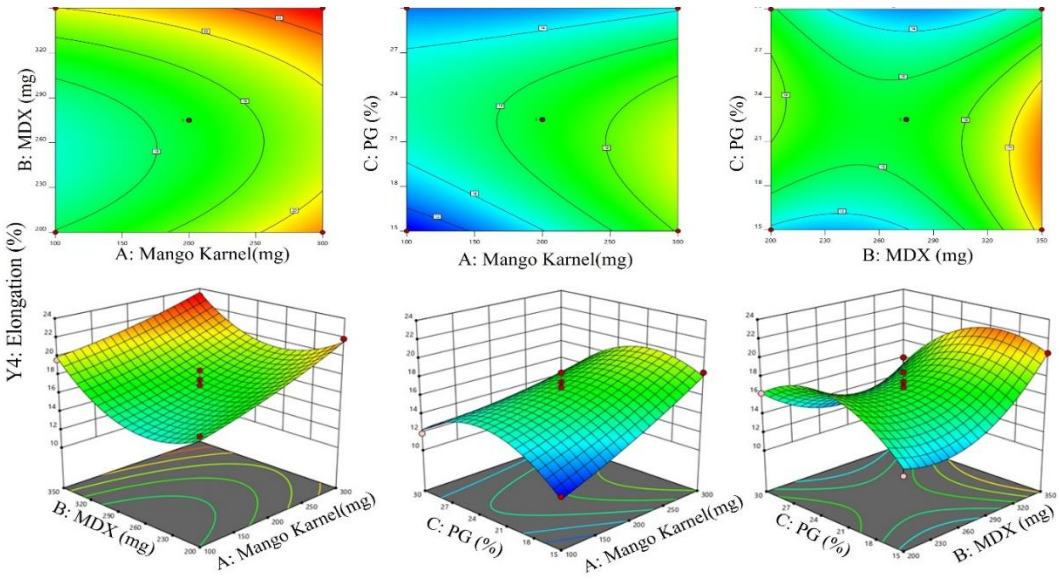

Fig. 5: Counter and response-surface-methodology plot for the effect of formulation factors (X1, X2, and X3) on the elongation (Y4)

Effect of formulation factors on dissolution

Fig. 6 shows the relatively consistent drug release profile across all formulations. The drug release from each formulation was greater than the disintegration values, with 90% being released within 15 min. The poor solubility of DMS in water is likely responsible for the observed release profile. Microparticles of the drug are disseminated throughout the water-soluble polysaccharide film matrix in rapidly dissolving films. Thus, DMS particle dissolution in a dissolution medium may coincide with film dissolution [68]. It was determined that mouth-dissolving films had a cumulative drug release in 5 min of 43.21±0.95 to 89.61±0.41%. The produced quadratic model showed that the Cumulative drug is significantly affected by the amounts of Mango kernel, Maltodextrin, and PG. As should be expected, there was a fair amount of concordance between the theoretical (predicted) values and the actual ones. With

an F-value of 75.63, it can be concluded that the mathematical model developed for the drug release in 5 min (Y5) is significant (Supplementary table 5).

Drug release studies =+76.12+2.60A+5.57B+6.60C+9.48AB-4.35AC+4.34BC-3.84A2-0.1990B2-16.81C2

Optimization by desirability function

A perturbation and desirability function optimization method was used to get the best results for each of the three possible responses. Tensile strength (Y1), disintegration time (Y2), folding endurance (Y3), elongation (Y4), and cumulative drug released in 5 min (Y5) responses were transformed into a disturbance and attraction scale. It was necessary to enhance Y1, while minimizing Y3, Y4, and Y5. The highest objective function (D) for each answer was determined by taking the maximum and minimum Y values, respectively. The Design-Expert program then performed a thorough grid search and feasibility search over the domain to get the global desirability value, which was the geometric mean of the individual desirability functions. At X1:300, X2:350, and X: 22.5, the highest values of the functions were found, respectively. Three batches of formulations were generated under the optimal composition, and the three responses were examined for each formulation to verify the model's capability for prediction. Since the anticipated and observed outcomes were in close agreement, the model was shown to be valid. The central composite design paired with a desirability function for evaluating and optimizing mouth-dissolving film compositions was successful, as the experimental values were extremely near to the anticipated values.

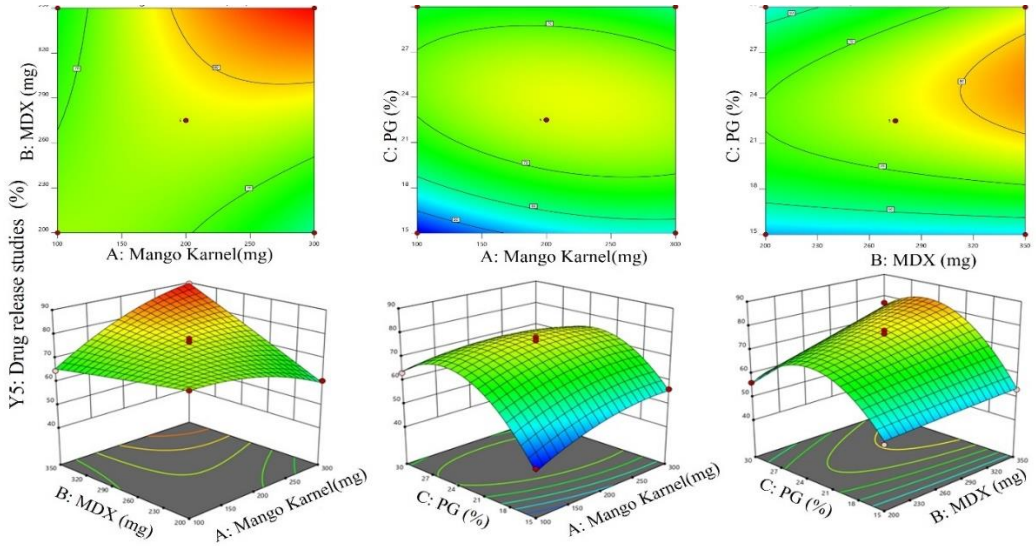

Fig. 6: Counter and response-surface-methodology plot for the effect of formulation factors (X1, X2, and X3) on the dissolution (Y5)

Two batches were chosen to test the disintegration time, thickness, and folding durability of using the overlay plot as a guide. Methods include measuring the drug's release over time, the tablet's tensile strength, its disintegration time, its folding endurance, its elongation, and its cumulative release. Tensile strengths of 8.96±0.02 and 7.85±0.05Mpa are shown for the F4 and F13 formulations, respectively, in fig. 7. With formula F4, disintegration happened in 15.34±1.24 seconds, but with formula F13, it took 16.35±2.46 seconds. The F4 formulation scored 354±2.41 on the folding endurance test, whereas the F13 variation scored 335±2.05. Extinction rates of 23.16±0.13 and 21.86±0.42% were calculated for Formulations F4 and F13, respectively. Results showed that F4's cumulative drug release was 89.61±0.48%, whereas F13 was only 79.48±1.48%. The results of tensile strength, disintegration time, folding endurance, elongation, and cumulative drug release tests on different batches are shown in table 4.

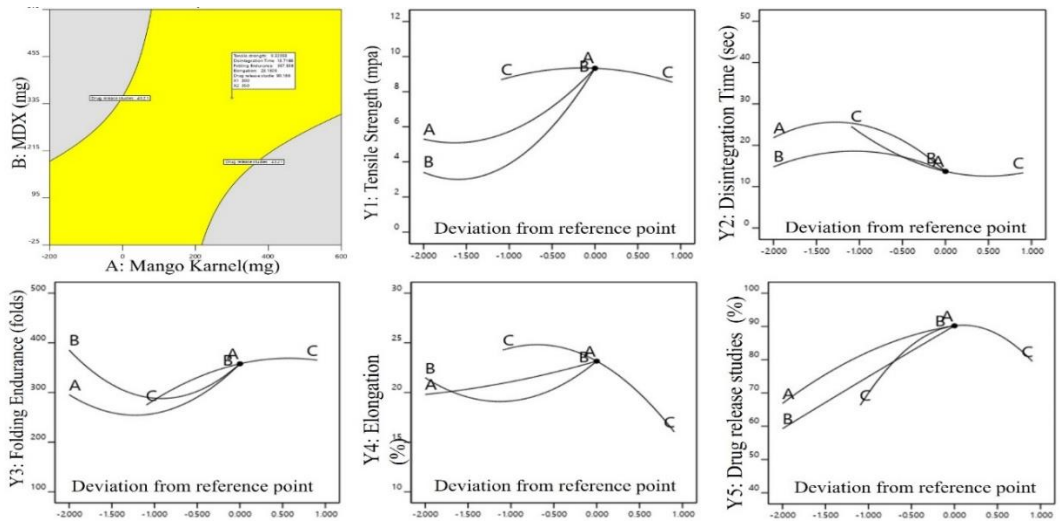

Fig. 7: Perturbation plots of dependent factors and overlay plot of optimized formulation

Table 4: Optimized values obtained by the constraints applies on Y1, Y2, Y3, Y4 and Y5

Variables	Optimum composition	Response	Observed value of response*	Predicted value of response	Percentage error
X1 (mg)	300	Y1	8.96±0.02	9.334	1.04
X2 (mg)	350	Y2	15.34±1.24	13.691	0.892
X3 (%)	22.5	Y3	354±2.41	357.858	1.010
		Y4	23.16±0.13	23.160	1
		Y5	89.61±0.48	90.207	1.006

*All the data are expressed as mean±standard deviation (n=3)

Pharmaceutical evaluation of films

There was a total of seventeen batches of Telmisartan-containing fast-dissolving oral thin films made. Mechanical and organoleptic qualities, including film thickness, dryness, tensile strength, folding durability, transparency, surface roughness, disintegration time, drug content, and surface pH, were analyzed for fast-dissolving films for oral administration.

Physical appearance/Texture

The films are glossy and clear, with a chic pink hue. The organoleptic properties of telmisartan films were evaluated, including their description, appearance, and Odor. Table 5 shows that it is transparent, odorless, and free of any floating particles or air bubbles.

Determination of weight variation

Studies on the weight fluctuation of each film guarantee that each patient receives the same dose of drug without any noticeable variations. Extreme variations in weight point to subpar quality control and nonuniform drug content throughout production. As non-uniform drug content would result in variable therapeutic impact, weight variation is a crucial component in determining therapeutic effectiveness. The film's density was determined using an electronic balance. We took three 2x2 cm samples of each formulation and weighed them on an analytical scale to determine their unique weights. Table 5 displays the results of a uniformity test conducted on drug-loaded films of 2 cm2 in size. The Effect of Fasting on Body Mass Index, The dissolving efficiency of films, was measured using the method outlined in the Section. The mass of mouth films that dissolve quickly ranges from 10.03±1.25 to 28.69±4.31. You can see the final weighted results in table 5. The concentration of the polymer has a linear effect on the mass of the substance. The film's steady rises in weight indicate that its many parts are being distributed uniformly.

Transparency

When placed in front of a black backdrop, it was discovered that all telmisartan OFDFs were completely see-through.

Table 5: Parameters used to assess oral rapid dissolving films containing telmisartan

F. No	Adhesiveness	Film clarity	Surface appearance	Drug content (%)	Weight (mg)	Av. pH±SD
1	Non-adhesive	Homogenous	Transparent	97.01±1.25	19.34±0.25	6.75±0.2
2	Non-adhesive	Homogenous	Transparent	98.36±0.96	18.52±0.13	7.03±0.1
3	Non-adhesive	Homogenous	Transparent	98.01±0.35	16.37±0.46	6.91±0.3
4	Non-adhesive	Homogenous	Transparent	99.87±1.24	23.03±1.25	6.82±0.1
5	Non-adhesive	Homogenous	Transparent	99.02±0.38	18.64±0.34	6.98±0.5
6	Non-adhesive	Homogenous	Transparent	98.63±0.75	15.34±1.10	6.94±0.4
7	Non-adhesive	Homogenous	Transparent	97.94±0.62	18.85±0.12	6.67±0.2
8	Non-adhesive	Homogenous	Transparent	98.31±0.15	16.32±2.34	6.79±0.2
9	Non-adhesive	Homogenous	Transparent	97.34±0.27	20.87±2.51	6.85±0.1
10	Non-adhesive	Homogenous	Transparent	98.15±1.03	24.31±0.36	7.01±0.4
11	Non-adhesive	Homogenous	Transparent	97.32±1.02	28.69±4.31	6.98±0.3
12	Non-adhesive	Homogenous	Transparent	98.34±1.13	17.01±2.18	7.06±0.1
13	Non-adhesive	Homogenous	Transparent	99.08±1.24	22.08±0.07	6.82±0.2
14	Non-adhesive	Homogenous	Transparent	97.34±0.49	20.39±0.54	6.79±0.2
15	Non-adhesive	Homogenous	Transparent	98.73±0.56	18.04±0.37	7.01±0.1
16	Non-adhesive	Homogenous	Transparent	97.82±0.38	18.38±0.85	7.35±0.4
17	Non-adhesive	Homogenous	Transparent	99.03±0.35	19.69±0.82	7.12±0.2

*All the data are expressed as mean±standard deviation (n=3)

Determination of drug content

Ten separate films were used to find out how to achieve content homogeneity. The film was 2 cm2 in size and was stored in a 100 ml volumetric flask. This was placed in a mechanical shaker and agitated until it dissolved, after which it was filtered to remove any remaining solids. After proper dilution, the drug was detected spectroscopically at 296 nm. For F1-F17. Oral quick-dissolving films' drug content was determined using the prescribed procedure. Oral rapid dissolving films were determined to have a drug concentration that was within the allowable range of values specified by IP, falling between 97.01±1.25 and 99.87±1.24. Table 5 displays the results of the drug content analysis. The amount of drug remaining in the film decreases with increasing film concentration and breakdown time. This measure provides useful context for the quantity of drug use shown in the picture.

Surface pH

Since the film will be dissolved in the mouth, its surface pH should be 6.8, the same as saliva, to prevent any irritation. Telmisartan's pH, determined in triplicate for each sample, ranged from 6.65 to 7.35, with an average of about pH 6.80; this was within the optimal range for use in the mouth. The approach was used to determine the surface pH of an orally dissolvable telmisartan film. The pH of the film's surface, which may be dissolved in the mouth, was determined to be between 6.67±0.2 and 7.35±0.4. (Supplementary table 6) displays the surface pH findings.

Thickness

Mango kernel, MDX, and PG were used to create a series of telmisartan oral film-dissolving films (OFDFs) with a thickness between 0.119±0.01 mm and 0.348±0.03 mm (formulations F1 through F17). Based on the measured thickness, it was found that a higher concentration of the film former resulted in a thicker film. Therefore, film thickness was proportional to the amount of film formers used. Oral quick dissolving film thickness was assessed using the established procedure. Oral quick-dissolving films were measured to have a thickness between 0.119±0.01 and 0.348±0.03.

The findings for the thickness may be shown in (Supplementary table 6) of the supplier catalogue. The greater the concentration of the polymer, the thicker the film. The thickness of the film is an important sign of how uniformly the drug was distributed.

Moisture loss and moisture uptake

The %moisture loss was determined after assessing the OFDFs that were developed. The % moisture loss in telmisartan films decreased from 8.240.13 to 3.63±0.34 when the polymer content changed. Studies on the polymer's ability to absorb water showed that as the polymer's concentration rose, so did its hydrophilicity (as shown in table 6 of the supplementary). This suggests that the polymer's increased hydrophilicity corresponds with its increased viscosity [69].

Solid state characterizations

Fourier transform infrared spectroscopic (FT-IR) analysis

C-N stretching vibrations at 1350-1100 cm-1, CH3 bending vibrations at 1455-1381 cm-1, the C-C aromatic band and stretching at 1599 cm-1, the C-H bending vibrations at 1460-1495 cm-1, and the C=O stretching vibrations at 1695 cm-1 were all detected as typical peaks in the infrared spectra of telmisartan. Both OH stretching (3300 cm-1) and OH bending (in-plane) modes (1635 cm-1) contribute to the two absorption bands seen in MDX spectra. The stretching band of CH absorption was measured to be at 2900 cm-1. The peaks in the PEG 400 spectra at 1145 and 962 cm-1 result from C-O stretching. Sorbitol spectra showed major absorption bands at 890, 1046, 1084, and 1411 cm-1. Pure Telmisartan FTIR spectra showed peaks at wavenumbers (cm-1) associated with the drug's functional groups. Telmisartan's ATR spectrum by itself. There was no interaction with the excipients since the free acid carbonyl peak of pure telmisartan, at 1692.14 cm-1`, was preserved in the solid dispersion. B-Cyclodextrin and HPMC were also shown to be effective in the solid dispersion-based formulation of mouth-dissolving films (supplementary fig. 1). Certain functional groups were detected as distinctive peaks in the FTIR spectra of telmisartan. Telmisartan is easily distinguished from other drugs because its ATR spectrum is unique.

Differential scanning calorimetry (DSC)

A temperature-induced phase transition causes telmisartan to melt at 78 °C, as seen by a sharp endothermic peak at this temperature. The phase shift occurred between 267 and 272 degrees Celsius. Mango kernel and telmisartan were shown to be physically compatible because the endotherm of telmisartan was properly preserved in its combination with mango kernel, MDX, and PG. Pure telmisartan's thermogram displays a distinct endothermic peak at its melting point of 269.68 degrees Celsius. This proves that the telmisartan is 100% pure and crystalline, as seen in Supplementary fig. 2. There was no evidence of interaction between telmisartan and excipients in thermo-grams of physical mixes of the drug and excipients (1:1). The drug's endothermic peak was only slightly shifted to a lower temperature or broadened in the improved formulation. It has been noted that the peak shape and enthalpy are affected by the amount of material utilized, particularly in drug-excipient mixes. Therefore, the combination of drug and excipient, which influences the purity of each component in the mixture, may account for these little variations in the melting endotherm of the drug, and may not necessarily signal possible incompatibility.

Powder X-ray diffractometry

Supplementary fig. 3 displays X-ray powder diffractograms for telmisartan, mango kernel, MDX, and the telmisartan-optimized formulation F4. Telmisartan was shown to be crystalline based on its powder X-ray diffractograms, which revealed strong peaks at diffraction angles between 13.74° and 37.8°. Within the diffraction angle range of 13.47° to 27.06°, the improved ezetimibe film showed a decrease in peak intensity (supplementary fig 3). The drug ezetimibe was transformed to an amorphous state after being formulated as a film with PG, as shown by a drastic decrease in the peak intensity in formulation F4. No distinct peaks can be seen in the pXRD data for the physical combination or the placebo film.

***In vitro* dissolution studies**

The findings of an *in vitro* drug release investigation utilizing fast-dissolving oral films containing telmisartan in both phosphate buffer (pH 6.8) and 0.1 N HCl solutions are shown in fig. 4 of the supplementary material. For the *in vitro* drug release study, we employed Franz diffusion cells with a dialysis membrane. There is a giving part and a receiving part. In the receptor area, 20 ml of phosphate buffer solution served as the diffusion medium. The resulting film was transferred to the receptor compartment, where magnetic beads rotated at a constant rate of 50 rpm while keeping the medium at 37.1 degrees Celsius. Using a JASCO V 530 spectrophotometer, 1 ml of receptor fluid was taken out at regular intervals and replaced with 1 ml of phosphate buffer solution before being analysed at 296 nm. Permitted total drug use over time was computed and graphed. The formulation's drug-release rate improved as mango kernel content rose. More than 60% of the drug was released after 10 min, across all batches (at pH 6.8). The creation of a complex from which drug releases more quickly at pH 6.8 might account for the variation in drug release across mediums (supplementary fig 4). These findings further demonstrated that the film formulation successfully concealed the bitter telmisartan flavor in the oral cavity [70].

Ex vivo drug permeation studies

Rat oral mucosa drug penetration experiments using optimum film and pure drug solution. When tested on rat oral mucosa, both optimized films (F4) and drug solution decomposed more slowly than in PBS solution, taking 15 and 8 min, respectively. You can see the increased penetration of Telmisartan-OFDFs (92.34%) and telmisartan (16.54%) over 30 min in the film with the improved formulation incorporating mango kernel in fig. Films on the oral mucosa did not disperse entirely after 3 h. (supplementary fig 5) depicts a potential new structure for mucoadhesive rapid dissolving films, Formulation F4, which may improve drug absorption via the oral mucosa [71].

Ex-vivo muco irritation by histological examination

Involvement of pain and inflammation is optional in the definition of irritation. The mucosal membrane is easily irritated because it contains glands that produce mucus, which is sticky and so attracts allergens. Before creating an oral drug delivery system, it is necessary to undertake oral mucosal irritation tests to assess the feasibility of this route for improved administration of the chosen drug. Oral quick-dissolving films may be harmful; thus, researchers are looking into that possibility using *in vitro* and/or *in vivo* testing procedures.

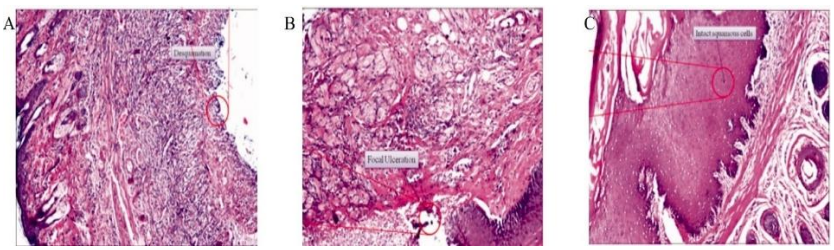

Fig. 8: Sections from rats treated with optimized oral fast-dissolving films (F4), rats treated with plain pure drug solution (a), and rats treated with the control group (b) at 100x magnification

Histological analysis was undertaken to determine the severity of the pathological alterations in tissue shape and organization brought on using bucco adhesive film. Fast-dissolving film should be harmless to the oral mucosa, with no side effects like those seen with controlled oral mucosa (redness, no irritation, no ulcers). Ex-vivo muco irritation was studied using eosin stain in this research, with the improved F4 formulation. Eosin is a luminous acidic molecule that stains dark red or pink when it attaches to positively charged components including proteins, collagen, and muscle fibers. Red blood cells are also strongly stained by eosin. This dye is the gold standard for histological research. The oral mucosa from a live sheep was used to conduct ex-vivo muco irritation. Fig. 8 displays the outcomes in comparison to untreated oral mucosa [72].

Pharmacokinetic studies

A validated HPLC method, developed in-house, was used to accurately measure telmisartan levels in the blood of rats. Supplementary table 7 summarizes the pharmacokinetic data, and fig. displays a plot of plasma concentrations vs time. The lowest mean Telmisartan plasma concentrations were seen after dosing with the aqueous solutions [73]. When compared to the AUC determined for the aqueous Telmisartan solution, the AUC was 30 times higher when Telmisartan was supplied as the oral rapid dissolving films. In comparison to the Cmax achieved with the same dosage of Telmisartan taken as an aqueous solution, the Cmax obtained with the optimized oral rapid dissolving films was 29.02-fold greater at 4.586 g/ml. Oral rapid dissolving films have the potential to have a larger Cmax without changing the Tmax (fig. 9) since the Tmax (35 min) after dosing was the same as that achieved inside aqueous solutions (35 min). These findings demonstrate that the oral fast-dissolving film formulation of Telmisartan significantly improves absorption compared to the aqueous suspensions [74].

Stability studies

Telmisartan oral rapid dissolving films' stability was investigated in this research. Three-month stability tests were conducted at 25±5 °C, 40±50C, and 75% RH. samples were tested for disintegration time, tensile strength, folding endurance, and *in vitro* dissolution at 0 d, 1 mo, and 3 mo. Table 6 displays the findings from the stability tests [75].

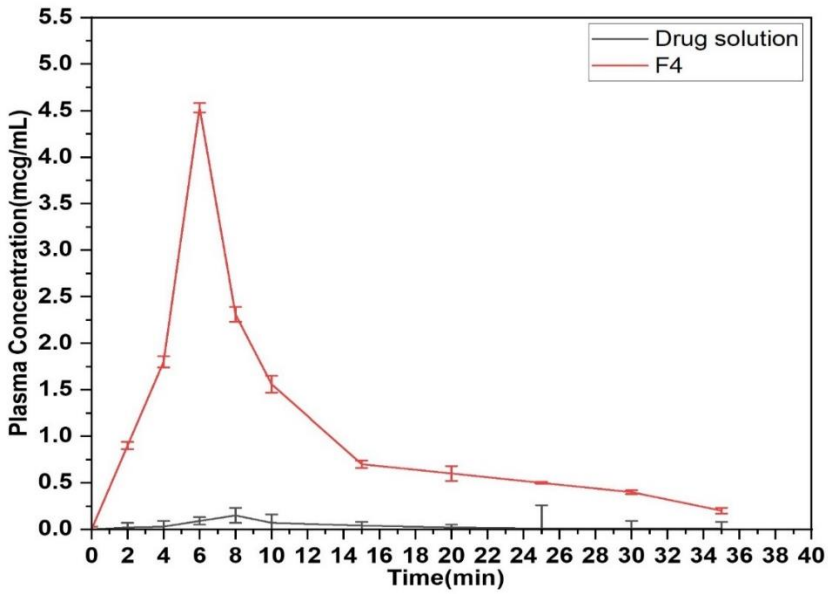

Fig. 9: Comparison of the pharmacokinetics of Telmisartan after oral administration of the oral quick dissolving film and the dosage aqueous solution

Table 6: Stability study of optimized oral fast dissolving films

Time	Physical appearance	Tensile strength	Folding endurance	Disintegration time	*In vitro* dissolution
Initial	Transparent	8.96±0.02	354±2.41	15.34±1.24	89.61±0.48
1 mo	Transparent	8.62±0.24	350±1.35	16.58±0.95	88.64±0.02
2 mo	Transparent	8.29±0.13	346±2.41	17.52±0.34	85.13±0.41
3 mo	Transparent	7.95±0.41	340±3.16	20.49±0.52	83.17±0.31

All the data are expressed as mean±standard deviation (n=3)

CONCLUSION

By developing a rapidly dissolving film for oral delivery, this study attempted to improve the solubility and bioavailability of TMS. OFDF for TMS was developed and refined with quality by design (QbD) in mind. The analysis of variance shows that the screening model used in the research provides a good match to the data. Furthermore, the prediction profile and the perturbation plot aid in determining which sets of elements would provide the desired outcomes. The right screening model was used in the experimentation thanks to the DoE software. FTIR, DSC, and XRD analyses have all shown that TMS is compatible with the excipients. Mango kernel, MDX, Aspartan, and PEG 400 were used in the development of TMS-OFDF. The solvent casting process is used to create OFDF, with a drug-to-carrier ratio of 1:1. Higher drug release was attributed to TMS and mango kernel OFDF. Additionally, the films were made using a solvent casting technique. Mango kernel, a film-forming polymer, was employed because it hydrates quickly. To hasten the disintegration process, a super disintegrant called PEG 400 was utilized. The films were evaluated based on several factors, including their thickness, folding durability, *in vitro* disintegration time, and *in vitro* dispersion investigations. Mango kernel, PG, and MDX were treated as independent variables in a Box-Behnken analysis with cumulative drug release and disintegration time as the dependent variables. It was found that 300 mg of mango kernel, 350 mg of MDX, and 23.213 % PG were the optimal amounts. The fourth iteration (F4) of the

optimized formulation of the drug was compared to the original drug solution *in vitro*, ex vivo, and pharmacokinetic studies. An ideal dosage form of telmisartan for the treatment of hypertension was created by combining mango kernel, a film-forming polymer, with MDX, a highly disintegrant oral dissolving film of TMS.

LIST OF ABBREVIATIONS

TMS=Telmisartan; OFDF=oral fast dissolving film; GIT=gastrointestinal tract; FTIR= Fourier transform infrared; FDF=Fast-dissolving film; CVD= cardiovascular disease; QbD=Quality by design; QTPP= Quality target product profile; CQAs= Critical quality attributes; CPPs= Critical process parameters; DSC=Differential scanning calorimetry; XRD= X-ray diffraction; CMAs= critical material attributes; HPLC=High performance Liquid Chromatography; DoE=Design of Experiment; BBD= Box-Behnken design; 2FI=two-factor interaction; ANOVA=Analysis of variance; EE=encapsulation efficiency; MDX= Maltodextrin; SEM= Scanning Electron Microscope; Sec =Seconds; mm= Millimeter; µm = micrometer; °C = degree centigrade; min= minutes; nm= nanometer; cm= centimeter; °C= degrees Celsius; Cmax=maximum concentration; Tmax= maximum concentration of time; AUCs= Areas under the curve; S=Significant; HS= highly significant; S/N= signal-to-noise ratio; PG= Propylene Glycol; %DR=Drug release percentage; SD= Standard deviation; DCM=dichloromethane; KBr=Potassium bromide; IAEC= Institute's Animal Ethics Committee; EU= European Union; USFDA=United States Food and Drug Administration; OECD= Organization for Economic Cooperation and Development; MRT= mean residence time; Cmax=maximum plasma concentration; tmax=maximum time; AUC=area under the curve; ICH=International conference of Harmonization

ETHICS APPROVAL AND CONSENT TO PARTICIPATE

The Institutional Animal Ethics Committee (IAEC) of Jeeva life sciences, Uppal, Hyderabad, India (Approval: CPCSEA/IAEC/JLS/011/11/22/15

AVAILABILITY OF DATA AND MATERIALS

Upon reasonable request, the associated author will make the utilized data and resources accessible.

FUNDING

This research received no external funding.

AUTHORS CONTRIBUTIONS

All the authors have contributed equally.

CONFLICT OF INTERESTS

The authors have no competing interests. No role was played by the funders in the study's conception, data's collection, analysis, or interpretation, or in the report's preparation or final publication.

REFERENCES

1. Alkahtani ME, Aodah AH, Abu Asab OA, Basit AW, Orlu M, Tawfik EA. Fabrication and characterization of fast-dissolving films containing escitalopram/quetiapine for the treatment of major depressive disorder. Pharmaceutics. 2021;13(6):891. doi: 10.3390/pharmaceutics13060891, PMID 34208460.
2. Dixit RP, Puthli SP. Oral strip technology: overview and future potential. J Control Release. 2009;139(2):94-107. doi: 10.1016/j.jconrel.2009.06.014, PMID 19559740.
3. Rowe RC, Sheskey P, Quinn M. Handbook of pharmaceutical excipients. Libros Digitales-Pharmaceutical Press; 2009.
4. Kulkarni AS, Deokule HA, Mane MS, Ghadge DM. Exploration of different polymers for use in the formulation of oral fast dissolving strips. J Curr Pharm Res. 2010;2(1):33-5.
5. Abruzzo A, Bigucci F, Cerchiara T, Cruciani F, Vitali B, Luppi B. Mucoadhesive chitosan/gelatin films for buccal delivery of propranolol hydrochloride. Carbohydr Polym. 2012;87(1):581-8. doi: 10.1016/j.carbpol.2011.08.024, PMID 34663007.
6. Aggarwal J, Singh G, Saini S, Rana AC. Fast dissolving films: a novel approach to oral drug delivery. Int Res J Pharm. 2011;2(12):69-71.
7. Jadhav SD, Kalambe RN, Jadhav CM, Tekade BW, Patil VR. Formulation and evaluation of fast-dissolving oral film of levocetirizine dihydrochloride. Int J Pharm Pharm Sci. 2012;4Suppl 1:337-41.
8. Shukla D. Mouth dissolving tablets I: an overview of formulation technology. Sci Pharm. 2009;77(2):309-26. doi: 10.3797/scipharm.0811-09-01.
9. Mashru RC, Sutariya VB, Sankalia MG, Parikh PP. Development and evaluation of fast-dissolving film of salbutamol sulphate. Drug Dev Ind Pharm. 2005;31(1):25-34. doi: 10.1081/ddc-43947, PMID 15704855.
10. Husain M, Agnihotri VV, Goyal SN, Agrawal YO. Development, optimization and characterization of hydrocolloid-based mouth dissolving film of telmisartan for the treatment of hypertension. Food Hydrocoll Health. 2022;2:100064. doi: 10.1016/j.fhfh.2022.100064.
11. Gondaliya K, Kapupara PP, Shah KV. Development and validation of RP-HPLC method for simultaneous estimation of clonidine hydrochloride and hydrochlorothiazide in pharmaceutical formulation. Int Boll Drug Res. 2014;4(6):106-15.
12. Vasseur B, Dufour A, Houdas L, Goodwin H, Harries K, Emul NY. Comparison of the systemic and local pharmacokinetics of clonidine mucoadhesive buccal tablets with reference clonidine oral tablets in healthy volunteers: an open-label randomised cross-over trial. Adv Ther. 2017;34(8):2022-32. doi: 10.1007/s12325-017-0585-9, PMID 28726169.
13. Gondkar SB, Namrata P, Saudagar RB. Fast dissolving oral films. Asian J Pharm Res. 2016;6(1):56-8.
14. Cunningham FE, Baughman VL, Peters J, Laurito CE. Comparative pharmacokinetics of oral versus sublingual clonidine. J Clin Anesth. 1994;6(5):430-3. doi: 10.1016/s0952-8180(05)80018-2, PMID 7986518.
15. Gilkeson GS, Delaney RL. Effectiveness of sublingual clonidine in patients unable to take oral medication. Drug Intell Clin Pharm. 1987;21(3):262-3. doi: 10.1177/106002808702100305, PMID 3569024.
16. Isaac J, Ganguly S, Ghosh A. Co-milling of telmisartan with poly(vinyl alcohol)–An alkalinizer free green approach to ensure its bioavailability. Eur J Pharm Biopharm. 2016;101:43-52. doi: 10.1016/j.ejpb.2016.01.016, PMID 26829378.
17. Segura J, Ruilope LM. A review of the benefits of early treatment initiation with single-pill combinations of telmisartan with amlodipine or hydrochlorothiazide. Vasc Health Risk Manag. 2013;9:521-8. doi: 10.2147/VHRM.S48291, PMID 24082785.
18. Meredith PA. Optimal dosing characteristics of the angiotensin II receptor antagonist telmisartan. Am J Cardiol. 1999;84(2A):7K-12K. doi: 10.1016/s0002-9149(99)00400-2, PMID 10437738.
19. Sangwai M, Vavia P. Amorphous ternary cyclodextrin nanocomposites of telmisartan for oral drug delivery: improved solubility and reduced pharmacokinetic variability. Int J Pharm. 2013;453(2):423-32. doi: 10.1016/j.ijpharm.2012.08.034, PMID 22935741.
20. Tran PHL, Tran HTT, Lee BJ. Modulation of microenvironmental pH and crystallinity of ionizable telmisartan using alkalizers in solid dispersions for controlled release. J Control Release. 2008;129(1):59-65. doi: 10.1016/j.jconrel.2008.04.001, PMID 18501462.
21. Borges AF, Silva BM, Silva C, Coelho JF, Simões S. Hydrophobic polymers for orodispersible films: a quality by design approach. Expert Opin Drug Deliv. (2016);13(10):1357-74. doi: 10.1080/17425247.2016.1218458, PMID 27466880.
22. Silva BMA, Vicente S, Cunha S, Coelho JFJ, Silva C, Reis MS. Retrospective quality by design (rQbD) applied to the optimization of orodispersible films. Int J Pharm. (2017);528(1-2):655-63. doi: 10.1016/j.ijpharm.2017.06.054, PMID 28629981.
23. Patil AS, Pethe AM. Quality by design (QbD): a new concept for development of quality pharmaceuticals. Int J Pharm Qual Assur. 2013;4(2):13-9.
24. Dangre PV, Phad RD, Surana SJ, Chalikwar SS. Quality by design (QbD) assisted fabrication of fast dissolving buccal film for clonidine hydrochloride: exploring the quality attributes. Adv Polym Technol. 2019;2019:1-13. doi: 10.1155/2019/3682402.
25. Chettupalli AK, Rao PA, Kuchukuntla M, Bakshi V. Development and optimization of aripiprazole ODT by using box-behnken

design. Res J Pharm Technol. 2020;13(12):6195-201. doi: 10.5958/0974-360X.2020.01080.X.
26. Cho HJ, Lee DW, Marasini N, Poudel BK, Kim JH, Ramasamy T. Optimization of self-microemulsifying drug delivery system for telmisartan using box–behnken design and desirability function. J Pharm Pharmacol. 2013;65(10):1440-50. doi: 10.1111/jphp.12115, PMID 24028611.
27. Amarachinta PR, Sharma G, Samed N, Chettupalli AK, Alle M, Kim JC. Central composite design for the development of carvedilol-loaded transdermal ethosomal hydrogel for extended and enhanced anti-hypertensive effect. J Nanobiotechnology. 2021;19(1):100. doi: 10.1186/s12951-021-00833-4, PMID 33836744.
28. Chettupalli AK, Ananthula M, Amarachinta PR, Bakshi V, Yata VK. Design, formulation, *in vitro* and ex-vivo evaluation of atazanavir loaded cubosomal gel. Biointerface res. J Appl Chem. 2021;11:12037-54.
29. Unnisa A, Chettupalli AK, Al Hagbani T, Khalid M, Jandrajupalli SB, Chandolu S. Development of dapagliflozin solid lipid nanoparticles as a novel carrier for oral delivery: statistical design, optimization, *in vitro* and *in vivo* characterization, and evaluation. Pharmaceuticals (Basel). 2022;15(5):568. doi: 10.3390/ph15050568, PMID 35631394.
30. Chettupalli AK, Rao PA, Kuchukuntla M, Bakshi V. Development and optimization of aripiprazole ODT by using box-behnken design. Res J Pharm Technol. 2020;13(12):6195-201. doi: 10.5958/0974-360X.2020.01080.X.
31. El-Setouhy DA, Abd El-Malak NSA. Formulation of a novel tianeptine sodium orodispersible film. AAPS PharmSciTech. 2010;11(3):1018-25. doi: 10.1208/s12249-010-9464-2, PMID 20532710.
32. Garg T, Murthy RSR, Kumar Goyal A, Arora S, Malik B. Development, optimization and evaluation of porous chitosan scaffold formulation of gliclazide for the treatment of type-2 diabetes mellitus. Drug Deliv Lett. 2012;2(4):251-61. doi: 10.2174/2210304x11202040003.
33. Kaur R, Garg T, Das Gupta U, Gupta P, Rath G, Goyal AK. Preparation and characterization of spray-dried inhalable powders containing nanoaggregates for pulmonary delivery of anti-tubercular drugs. Artif Cells Nanomed Biotechnol. 2016;44(1):182-7. doi: 10.3109/21691401.2014.930747, PMID 24992699.
34. Prasad RR, Kumar JR, Vasudha B, Kumar CA. Formulation development and evaluation of allopurinol solid dispersions by solvent evaporation technique. Int J App Pharm. 2018;10(4):168-71. doi: 10.22159/ijap.2018v10i4.25311.
35. Cunningham FE, Baughman VL, Peters J, Laurito CE. Comparative pharmacokinetics of oral versus sublingual clonidine. J Clin Anesth. 1994;6(5):430-3. doi: 10.1016/s0952-8180(05)80018-2, PMID 7986518.
36. Beg S, Al Robaian M, Rahman M, Imam SS, Alruwaili N, Panda SK. editors. Pharmaceutical drug product development and process optimization: effective use of quality by design. CRC Press; 2020.
37. Yir-Erong B, Bayor MT, Ayensu I, Gbedema SY, Boateng JS. Oral thin films as a remedy for noncompliance in pediatric and geriatric patients. Ther Deliv. 2019;10(7):443-64. doi: 10.4155/tde-2019-0032, PMID 31264527.
38. Irfan M, Rabel S, Bukhtar Q, Qadir MI, Jabeen F, Khan A. Orally disintegrating films: a modern expansion in drug delivery system. Saudi Pharm J. 2016;24(5):537-46. doi: 10.1016/j.jsps.2015.02.024, PMID 27752225.
39. Nalluri BN, Sravani B, Anusha VS, Sribramhini R, Maheswari KM. Development and evaluation of mouth dissolving films of sumatriptan succinate for better therapeutic efficacy. J Appl Pharm Sci. 2013;3(8):161-6.
40. Rani KC, Parfati N, Aryani NLD, Winantari AN, Fitriani EW, Pradana AT. Development, evaluation, and molecular docking of oral dissolving film of atenolol. Pharmaceutics. 2021;13(10):1727. doi: 10.3390/pharmaceutics13101727, PMID 34684021.
41. Hussain A, Latif S, Abbas N, Irfan M, Arshad MS, Bukhari NI. Hydroxypropyl cellulose-based orally disintegrating films of promethazine HCl for the treatment of motion sickness. Trop J Pharm Res. 2018;17(6):991-6. doi: 10.4314/tjpr.v17i6.2.
42. Satyanarayana DA, Keshavarao KP. Fast disintegrating films containing anastrozole as a dosage form for dysphagia patients. Arch Pharm Res. 2012;35(12):2171-82. doi: 10.1007/s12272-012-1215-3, PMID 23263812.
43. Avula PR, Chettupalli AK, Chauhan V, Jadi RK. Design, formulation, *in vitro* and *in vivo* pharmacokinetic evaluation of nicardipine-nanostructured lipid carrier for transdermal drug delivery system. Mater Today Proc. 2023.
44. Unnisa A, Chettupalli AK, Alazragi RS, Alelwani W, Bannunah AM, Barnawi J. Nanostructured lipid carriers to enhance the bioavailability and solubility of ranolazine: statistical optimization and pharmacological evaluations. Pharmaceuticals (Basel). 2023;16(8):1151. doi: 10.3390/ph16081151, PMID 37631066.
45. Sameina LH, Idamakantia S, Chettupalli AK, Velamala RR, Ezzat MO. Design of mesalamine loaded micro-particles: Preparation, *in vitro* and *in vivo* characterization. Mater Today Proc. 2023. doi: 10.1016/j.matpr.2023.07.063.
46. Dandamudi SP, Chettupalli AK, Dargakrishna SP, Nerella M, Amara RR, Yata VK. Response surface method for the simultaneous estimation of atorvastatin and olmesartan. Trends Sci. 2022;19(18):5799. doi: 10.48048/tis.2022.5799.
47. Samprasit W, Akkaramongkolporn P, Kaomongkolgit R, Opanasopit P. Cyclodextrin-based oral dissolving films formulation of taste-masked meloxicam. Pharm Dev Technol. 2018;23(5):530-9. doi: 10.1080/10837450.2017.1401636, PMID 29103353.
48. Maher EM, Ali AMA, Salem HF, Abdelrahman AA. *In vitro*/*in vivo* evaluation of an optimized fast dissolving oral film containing olanzapine co-amorphous dispersion with selected carboxylic acids. Drug Deliv. 2016;23(8):3088-100. doi: 10.3109/10717544.2016.1153746, PMID 26960680.
49. Shen BD, Shen CY, Yuan XD, Bai JX, Lv QY, Xu H. Development and characterization of an orodispersible film containing drug nanoparticles. Eur J Pharm Biopharm. 2013;85(3 Pt B):1348-56. doi: 10.1016/j.ejpb.2013.09.019, PMID 24103635.
50. Mashru RC, Sutariya VB, Sankalia MG, Parikh PP. Development and evaluation of fast-dissolving film of salbutamol sulphate. Drug Dev Ind Pharm. 2005;31(1):25-34. doi: 10.1081/ddc-43947, PMID 15704855.
51. Kumar AC, Prathap M, Venketeswararao P, Babu AS, Babu RN, Shanthi MS. Development of itraconazole immediate release pellets by using HPMC loaded in gelatin capsules. Int J Biol Pharm Res. 2012;3(7):904-5.
52. Kaur M, Malik B, Garg T, Rath G, Goyal AK. Development and characterization of guar gum nanoparticles for oral immunization against tuberculosis. Drug Deliv. 2015;22(3):328-34. doi: 10.3109/10717544.2014.894594, PMID 24611942.
53. Semalty M, Semalty A, Kumar G. Formulation and characterization of mucoadhesive buccal films of glipizide. Indian J Pharm Sci. 2008;70(1):43-8. doi: 10.4103/0250-474X.40330, PMID 20390079.
54. Modgill V, Garg T, Goyal AK, Rath G. Permeability study of ciprofloxacin from ultra-thin nanofibrous film through various mucosal membranes. Artif Cells Nanomed Biotechnol. 2016;44(1):122-7. doi: 10.3109/21691401.2014.924007, PMID 24915047.
55. Weibel ER, Bacigalupe LD, Schmitt B, Hoppeler H. Allometric scaling of maximal metabolic rate in mammals: muscle aerobic capacity as determinant factor. Respir Physiol Neurobiol. 2004;140(2):115-32. doi: 10.1016/j.resp.2004.01.006, PMID 15134660.
56. West GB, Brown JH. The origin of allometric scaling laws in biology from genomes to ecosystems: towards a quantitative unifying theory of biological structure and organization. J Exp Biol. 2005;208(9):1575-92. doi: 10.1242/jeb.01589, PMID 15855389.
57. Abou el Ela AESF, Allam AA, Ibrahim EH. Pharmacokinetics and anti-hypertensive effect of metoprolol tartrate rectal delivery system. Drug Deliv. 2016;23(1):69-78. doi: 10.3109/10717544.2014.904021, PMID 24758140.
58. El Sayeh A, Abou el Ela F, Ibrahim EH, Allam AA. Bucco-adhesive tablets containing metoprolol tartarate: formulation, *in vitro* and *in vivo* characterization. J Drug Deliv Sci Technol. 2013;23(2):171-9. doi: 10.1016/S1773-2247(13)50026-8.

59. Sastry MSP, Satyanarayana NV, Diwan PV, Krishna DR. Formulation, phafmacokinetic and pharmacodynamic evaluation of fast releasing compressed propranolol. HCL suppositories. Drug Dev Ind Pharm. 1993;19(9):1089-96. doi: 10.3109/03639049309063003.
60. El-Feky YA, Mostafa DA, Al-Sawahli MM, El-Telbany RFA, Zakaria S, Fayez AM. Reduction of intraocular pressure using timolol orally dissolving strips in the treatment of induced primary open-angle glaucoma in rabbits. J Pharm Pharmacol. 2020;72(5):682-98. doi: 10.1111/jphp.13239, PMID 32170884.
61. Liu C, Chang D, Zhang X, Sui H, Kong Y, Zhu R. Oral fast-dissolving films containing lutein nanocrystals for improved bioavailability: formulation development, *in vitro* and *in vivo* evaluation. AAPS PharmSciTech. 2017;18(8):2957-64. doi: 10.1208/s12249-017-0777-2, PMID 28462465.
62. Lai KL, Fang Y, Han H, Li Q, Zhang S, Li HY. Orally-dissolving film for sublingual and buccal delivery of ropinirole. Colloids Surf B Biointerfaces. 2018;163:9-18. doi: 10.1016/j.colsurfb.2017.12.015, PMID 29268211.
63. Londhe V, Shirsat R. Formulation and characterization of fast-dissolving sublingual film of iloperidone using box–behnken design for enhancement of oral bioavailability. AAPS PharmSciTech. 2018;19(3):1392-400. doi: 10.1208/s12249-018-0954-y, PMID 29396734.
64. Abd El Azim H, Nafee N, Ramadan A, Khalafallah N. Liposomal buccal mucoadhesive film for improved delivery and permeation of water-soluble vitamins. Int J Pharm. 2015;488(1-2):78-85. doi: 10.1016/j.ijpharm.2015.04.052, PMID 25899288.
65. Bermudez Oria A, Rodriguez Gutierrez G, Vioque B, Rubio Senent F, Fernandez Bolaños J. Physical and functional properties of pectin-fish gelatin films containing the olive phenols hydroxytyrosol and 3,4-dihydroxyphenylglycol. Carbohydr Polym. 2017;178:368-77. doi: 10.1016/j.carbpol.2017.09.042, PMID 29050607.
66. Junmahasathien T, Panraksa P, Protiarn P, Hormdee D, Noisombut R, Kantrong N. Preparation and evaluation of metronidazole-loaded pectin films for potentially targeting a microbial infection associated with periodontal disease. Polymers. 2018;10(9):1021. doi: 10.3390/polym10091021, PMID 30960947.
67. Raza SN, Kar AH, Wani TU, Khan NA. Formulation and evaluation of mouth dissolving films of losartan potassium using 3^2 factorial design. Int J Pharm Sci Res. 2019;10(3):1402-11.
68. Yir-Erong B, Bayor MT, Ayensu I, Gbedema SY, Boateng JS. Oral thin films as a remedy for noncompliance in pediatric and geriatric patients. Ther Deliv. 2019;10(7):443-64. doi: 10.4155/tde-2019-0032, PMID 31264527.
69. Hussain A, Latif S, Abbas N, Irfan M, Arshad MS, Bukhari NI. Hydroxypropyl cellulose-based orally disintegrating films of promethazine HCl for the treatment of motion sickness. Trop J Pharm Res. 2018;17(6):991-6. doi: 10.4314/tjpr.v17i6.2.
70. Adrover A, Varani G, Paolicelli P, Petralito S, Di Muzio L, Casadei MA. Experimental and modeling study of drug release from HPMC-based erodible oral thin films. Pharmaceutics. 2018;10(4):222. doi: 10.3390/pharmaceutics10040222, PMID 30423941.
71. Akyuz L, Duman F, Kaya M. Encapsulation of flurbiprofen by chitosan using a spray-drying method with *in vitro* drug releasing and molecular docking. Turk J Pharm Sci. 2017;14(1):34-9. doi: 10.4274/tjps.95867, PMID 32454592.
72. Shah J, Patel S, Bhairy S, Hirlekar R. Formulation optimization, characterization and *in vitro* anti-cancer activity of curcumin loaded nanostructured lipid carriers. Int J Curr Pharm Sci. 2022;14(1):31-43. doi: 10.22159/ijcpr.2022v14i1.44110.
73. Kaczmarek B. Improving sodium alginate films properties by phenolic acid addition. Materials (Basel). 2020;13(13):2895. doi: 10.3390/ma13132895, PMID 32605181.
74. Centkowska K, Ławrecka E, Sznitowska M. Technology of orodispersible polymer films with micronized loratadine-influence of different drug loadings on film properties. Pharmaceutics. 2020;12(3):250. doi: 10.3390/pharmaceutics12030250, PMID 32164345.
75. Ouda GI, Dahmash EZ, Alyami H, Iyire A. A novel technique to improve drug loading capacity of fast/extended release orally dissolving films with potential for paediatric and geriatric drug delivery. AAPS PharmSciTech. 2020;21(4):126. doi: 10.1208/s12249-020-01665-5, PMID 32382992.